This is a preproof accepted article for *Mineralogical Magazine*
This version may be subject to change during the production process
DOI: 10.1180/mgm.2025.10184

Steric contribution in compressibilities of K^+ coordination polyhedra

Sergey V. Rashchenko[1,2,*]

[1]Sobolev Institute of Geology and Mineralogy, Siberian Branch of Russian Academy of Sciences, 3 Koptyuga Avenue, 630090, Novosibirsk, Russia

[2]Novosibirsk State University, 1 Pirogova Street, 630090, Novosibirsk, Russia

*rashchenko@igm.nsc.ru

Abstract

The bulk modulus of a crystal is often closely related to the compressibility of its constituent elements, such as cation-centered coordination polyhedra. The compressive behavior of regular polyhedra with a fixed coordination number was thoroughly studied decades ago and was found to follow a simple universal rule. However, the compressive behavior of large cations with irregular and poorly defined coordination polyhedra has not been systematically studied due to several methodological challenges and biases. Here, an original approach to defining and analyzing polyhedral compressibility is proposed, based on the concepts of effective coordination number (ECoN) and weighted mean bond length. This approach is demonstrated using K^+ coordination polyhedra as an example.

Keywords: pressure; polyhedron; compressibility; bulk modulus; effective coordination number; *ECoN*; weighted mean bond length

Introduction

The effect of high pressure on inorganic and mineral structures has traditionally been quantified using the combination of mutual rotation of coordination polyhedra and their deformation. While the polyhedral rotation schemes are largely specific to the structure, the pressure-induced deformation of individual coordination polyhedra follows more universal principles. The first attempt to formulate these principles was made in 1977 by Hazen and Prewitt (Hazen and Prewitt, 1977). They empirically found that cation-oxygen polyhedra can be described by a constant $K \cdot r^3/z_c$ ratio, where z_c is the formal charge of the cation, r is the mean bond length and K is the bulk modulus of the polyhedron. Later, Hazen and Finger extended this observation to include cations in halides, chalcogenides, pnictides and carbides, by incorporating

'ionicity' (S^2, 0.5 for coordination by oxygen) and anion charge (z_a) into the formula (Hazen and Finger, 1979). The resulting trend

$$\frac{K \cdot r^3}{S^2 z_c z_a} = 750(20)\text{GPa} \cdot \text{Å}^3 \quad (1)$$

has since been widely used as a reference in high-pressure crystal chemistry. However, it should be noted that the empirical data used by Hazen and Finger to derive Eq. 1 was limited to the compression behavior of regular polyhedra with a fixed coordination number of four, six and eight, which were described for compounds with relatively simple and symmetric crystal structures (e.g., NaCl, cubic ZnS, fluorite, garnet).

A major issue that has not been adequately addressed until now is the extension of the universal compressibility rule to the cases where: (1) polyhedra undergo a continuous change in coordination number under pressure, and (2) polyhedra have a large coordination number an ill-defined limit of the first coordination shell.

These cases are particularly relevant for 'large cations' (K^+, Ba^{2+} etc.), and the example of K^+ is particularly relevant to Earth science and has been relatively well studied under high-pressure. This example will be discussed in more detail below.

Data sources

The sources of crystallographic data used for the analysis of K^+ polyhedral compressibility are listed in Table 1. For the most of the crystal structures considered, the K^+ content at the corresponding crystallographic sites exceeds 90 mol. %. Two exceptions are the crystal structures of fluorapophyllite-(K) and nepheline, which have site stoichiometries of $K_{0.70}(NH_4)_{0.20}Na_{0.07}\square_{0.10}$ and $K_{0.54}Na_{0.24}Ca_{0.03}\square_{0.22}$, respectively. None of the crystal structures show positional disorder in either the K^+ sites or the ligands that coordinate them. The data in CIF format was downloaded either as electronic supplementary materials to original publications or from the American Mineralogist Crystal Structure Database (Downs and Hall-Wallace, 2003) or was kindly provided by the authors. Where necessary, the _cell_measurement_pressure key with corresponding pressure values was added to the original CIF files for further machine processing. In cases where no pressure uncertainty was reported, a value of 0.05 GPa was used. The data was processed using the graphical user interface of the crystchemlib Python library (Rashchenko, 2025), in accordance with the following procedure:

(1) For each K^+ site in each dataset, an effective coordination number (*ECoN*) vs. pressure (*P*) plot was generated, considering K–O distances up to 4 Å.

https://doi.org/10.1180/mgm.2025.10184 Published online by Cambridge University Press

(2) In each case, a pressure range with a constant d(*ECoN*) / d*P* slope was selected as the working range for further calculations. The values of d(*ECoN*) / d*P* slope and the intersection ($ECoN_0$) were then fitted by a linear function.

(3) With the selected pressure range, a plot of weighted mean bond length (*r*) vs. pressure was generated, considering K–O distances up to 4 Å. The r^3 value, which serves as as a proxy for polyhedral volume compressibility, was then fitted with a second order Birch-Murnaghan equation of state to obtain the r_0^3 and K_0 (bulk modulus) values. Least squares fitting was performed using the scipy.odr Python module, implemented in the crystchemlib graphical user interface.

For more information on the definition of *ECoN* and weighted mean bond length, please see below.

Table 1. Sources of crystallographic data used for analysis of K^+ polyhedra compressibility

	Site	Occupancy	P_{max}, GPa*	$ECoN_0$	d(*ECoN*) / d*P*, GPa^{-1}	r_0^3, $Å^3$	K_0, GPa	Key**
α-$K_2Ca_3(CO_3)_4$ (Ignatov et al., 2024)	K1	$K_{1.00}$	6.3	8.548(7)	–0.006(3)	22.72(3)	32.3(7)	a
	K3	$K_{1.00}$	6.3	8.383(16)	0.048(5)	23.64(5)	41.6(14)	b
Kokchetavite (Romanenko et al., 2024)	K1	$K_{0.96}□_{0.04}$	5.3	12.0(5)	–0.93(16)	30.9(5)	6.3(6)	c
	K2	$K_{0.96}□_{0.04}$	5.3	10.83(16)	–0.53(5)	29.2(3)	10.6(9)	d
Hydroxylapophyllite-(K) (Seryotkin, 2024)	K	$K_{0.96}□_{0.04}$	2.7	8	0	25.80(4)	18.1(6)	e
Fluorapophyllite-(K) (Seryotkin and Ignatov, 2023)	K	$K_{0.70}(NH_4)_{0.20}Na_{0.07}□_{0.10}$	4.3	8	0	26.44(5)	21.9(8)	f
Leucite (Gatta et al., 2008)	KK	$K_{0.95}Na_{0.03}□_{0.02}$	1.8	8.02(6)	–0.47(6)	29.5(3)	11.9(17)	g
Nepheline (Gatta and Angel, 2007)	K	$K_{0.54}Na_{0.24}Ca_{0.03}□_{0.22}$	4.1	11.01(6)	–0.27(3)	28.69(12)	17.4(9)	h
Phlogopite (1*M*) (Comodi et al., 2004)	K	$K_{0.91}Na_{0.02}Ba_{0.03}□_{0.04}$	5.0	10.30(12)	–0.46(4)	29.3(7)	12(3)	i
Microcline (Allan and Angel, 1997)	KM	$K_{0.97}Na_{0.01}□_{0.02}$	6.2	8.82(3)	–0.134(7)	25.26(9)	24.6(11)	j

*Pressure range of constant d(*ECoN*) / d*P*

**In Figs. 6-7

Definition of polyhedron compressibility

https://doi.org/10.1180/mgm.2025.10184 Published online by Cambridge University Press

For regular polyhedra with a fixed coordination number, such as those analysed by Hazen and Finger to derive Eq. 1, the definition of volume compressibility is straightforward and relates directly to the pressure-induced change in polyhedron volume, which is fitted with a suitable equation of state. However, for more complex cases, as outlined in the Introduction, a more detailed approach is required. This will be illustrated below using the example of kokchetavite, a hexagonal polymorph of $KAlSi_3O_8$, which was studied under high pressure by (Romanenko et al., 2024).

In the pressure range between 0.3 and 10.4 GPa, the kokchetavite structure adopts the *P*–6*c*2 space group and contains two potassium sites, K1 and K2, sandwiched between six-membered rings of aluminosilicate tetrahedra. At pressures near 0.3 GPa, the rings surrounding the K1 site have a close to regular hexagonal shape (Fig. 1a), so the K^+ cation is coordinated by 12 oxygen atoms of six O11 and six O12 sites, with a minor difference between K1–O11 and K1–O12 bond lengths. However, as pressure increases, the six-membered aluminosilicate rings become progressively distorted in a ditrigonal manner (Fig. 1b). This causes the six K1–O11 bond lengths to increase from ~3.1 to ~3.3 Å, while the six K1–O12 bond lengths decrease from ~3.0 to ~2.6 Å.

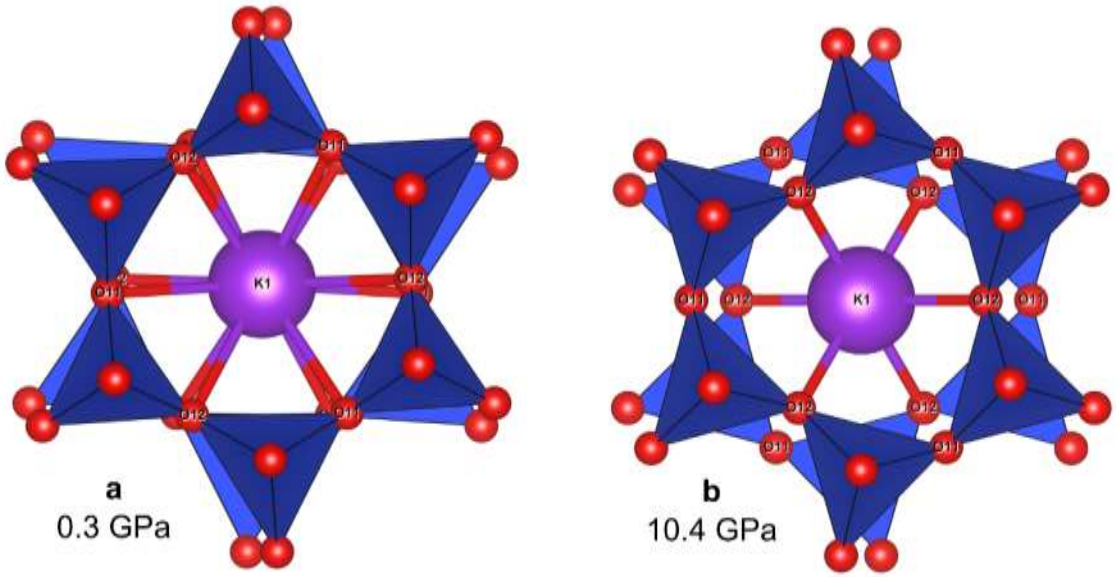

Figure 1. Coordination of the K1 site in the kokchetavite structure by six-membered rings of aluminosilicate tetrahedra at different pressures

The evolution of the K1–O11 and K1–O12 bond lengths, as shown in Fig. 2a, leads to an ambiguous definition of the coordination polyhedron around the K1 site. At 0.3 GPa, the K1 site

https://doi.org/10.1180/mgm.2025.10184 Published online by Cambridge University Press

has 12 neighbours in the form of a hexagonal prism, as seen in Fig. 1a. However, at 10.4 GPa, the O11 sites, which are located ~3.3 Å from the K1 site, barely enter the first coordination sphere, which is formed by six short (~2.6 Å) contacts with the O12 sites. This results in a coordination number of '6 + 6' (distorted hexagonal prism, Fig. 1b) or even as octahedral coordination for K1.

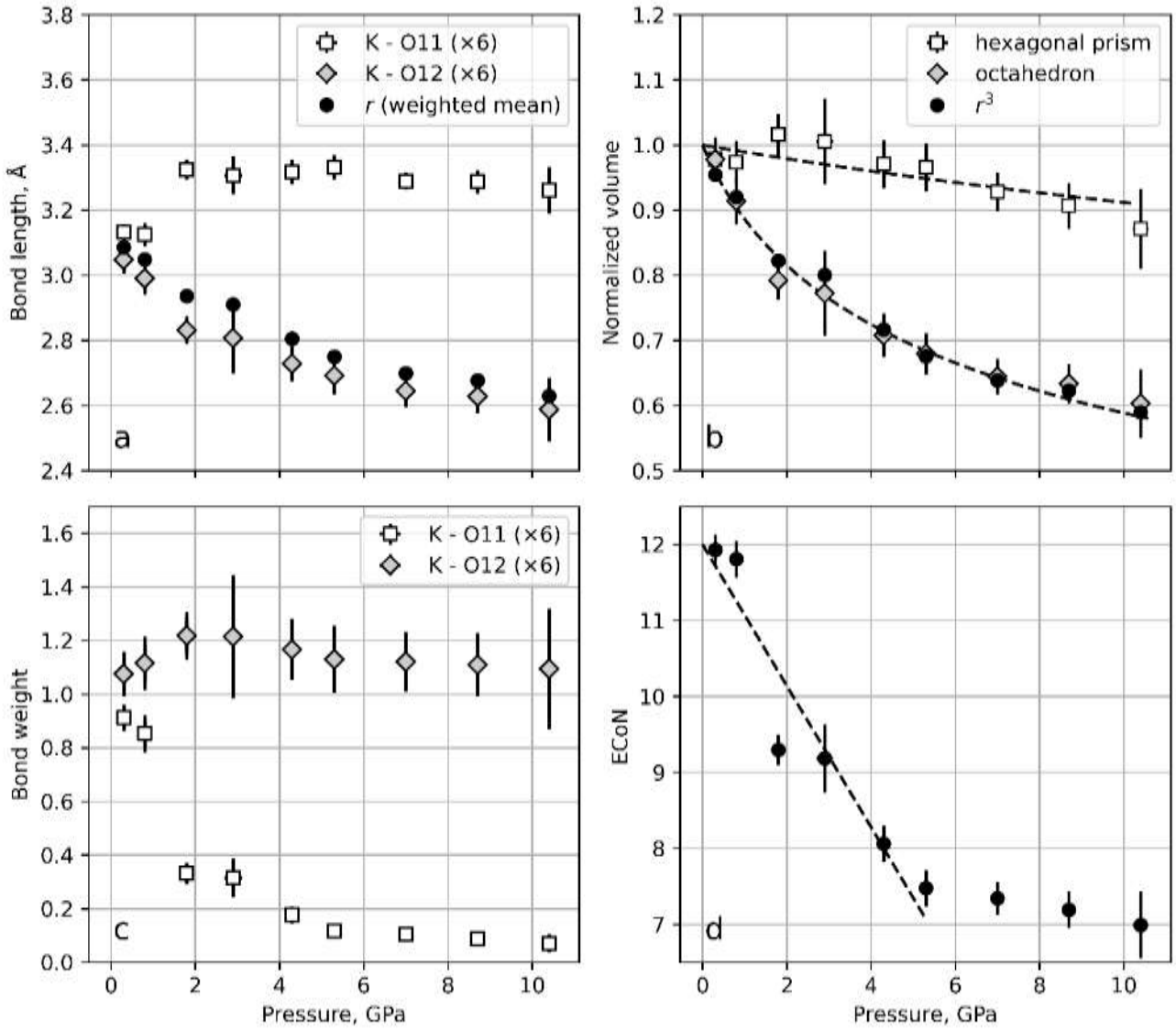

Figure 2. The parameters of the K1 site coordination polyhedron in the kokchetavite structure under compression. The dashed lines represent the least squares fit using a second-order Birch-Murnaghan equation of state (b) and a linear function between 0.3 and 5.3 GPa (d).

Surprisingly, when considering the K1 polyhedron as a hexagonal prism (nearly regular at 0.3 GPa and progressively distorted with increasing pressure), it is found that its volume exhibits

https://doi.org/10.1180/mgm.2025.10184 Published online by Cambridge University Press

an unphysical volume vs. pressure curve (Fig. 2b) and an unrealistically high bulk modulus of about 90 GPa. The latter reflects a dominant contribution from the six outer O11 ligands in the polyhedron volume, with K1–O11 bonds that are nearly independent of pressure (Fig. 2a). However, this behaviour is not due to the rigidity of the K1–O11 bond, but rather to the weakening of these bonds and the 'expulsion' of the six O11 ligands from the first coordination sphere. This weakening of the K1–O11 bonds can be quantified by calculating bond weights in the K1 polyhedron (Hoppe, 1979; Nespolo et al., 1999), which correspond to the contribution of each bond to the effective coordination number (*ECoN*). Fig. 2c shows that the bond weights of K1–O11 bonds gradually decrease from ~0.9 to ~0.1 over the pressure range of 0.3–5.3 GPa, while the bond weights of K1–O12 remain between 1.1 and 1.2 over the entire studied pressure range. This has an important consequence: the effective coordination number of the K1 site decreases from ~12 to ~7.5 over the 0.3–5.3 GPa pressure range in a quasi-linear manner (Fig. 2d; a discontinuity between 0.8 and 1.8 GPa is likely due to a subtle structural transformation that was overlooked in the original publication). At higher pressures, the negative d*ECoN* / d*P* slope becomes gentler, indicating a change in the compressive behaviour of the structure.

At first glance, the observed behaviour of K1 effective coordination number appears counter-intuitive, as most of crystallography and mineralogy textbooks traditionally state that higher pressure should promote an increase in coordination number. While this may be true for textbook examples such as the four-fold to six-fold coordination changes of silicon and aluminium in high-pressure aluminosilicates, it does not necessarily apply to larger cations with their distinct crystal chemistry. Instead, a more fundamental principle to consider is Pauling's first rule, which states that coordination number depends on the ratio of ionic radii. In the context of high pressure crystal chemistry, this can be rephrased as: under compression, the coordination number tends to increase for less compressible cations and decrease more compressible cations compared to anions. Such a formulation readily explains both the increase in the coordination number of silicon and aluminium in high-pressure aluminosilicates (since Si^{4+} and Al^{3+} cations are less compressible than the O^{2-} anion) and the decrease in the coordination number of potassium in kokchetavite discussed above (since the K^{+} cation is more compressible than the O^{2-} ligands). The corresponding changes in the coordination sphere hence demonstrate the following features:

https://doi.org/10.1180/mgm.2025.10184 Published online by Cambridge University Press

(1) when the central cation is less compressible than the ligand anions, upon compression, its first coordination shell tends to expand, accommodating additional ligands from the outer coordination spheres

(2) when the central cation is more compressible than the ligands, upon compression, the coordination shell splits into two subshells: one collapses to form a new lower-coordination polyhedron, while the ligands of the other are expelled outside.

The latter feature does indeed occur in the case of K1 coordination in kokchetavite (Fig. 2a), which explains why considering O11 ligands in the analysis of polyhedral compressibility leads to such unphysical results. Instead, one could consider only the six nearest O12 ligands in the K1 coordination polyhedron. The volume of the resulting octahedron shows much more realistic behaviour with a bulk modulus of ~6.5 GPa (Fig. 2b), as it reflects the properties of the most significant short K1–O12 bonds. This consideration, which is quite reliable at higher pressures, is questionable below 5.3 GPa, where the contribution of completely ignored O11 ligands to *ECoN* is certainly not negligible (Fig. 2c).

Therefore, polyhedra with pressure-induced continuous changes in coordination present a particular challenge for formalizing the definition of polyhedral compressibility. As more ligands are taken into account, the volume of the polyhedron does not reflect the actual bonding interactions. Otherwise, it does not account for the significant contribution of certain ligands. Attempting to divide the studied pressure range into segments based on different geometries of the coordination polyhedron would hinder the analysis of volume compressibility, which requires a continuous volume vs. pressure curve. It would also require a somewhat arbitrary and often meaningless decision on the precise pressure values at which one geometry transitions into another.

To address the above issue, one can use the weighted mean bond length (hereafter r) as a measure of the linear extent of the coordination polyhedron. This automatically accounts for the contribution of each ligand to *ECoN*, and the weights used in the averaging correspond to the bond weights introduced above. The contribution of the closest ligands dominates the result, as can be seen in Fig. 2a, which shows the calculation of r for the K1 polyhedron in the kokchetavite structure. The value of r is close to the six shortest K1–O12 bond lengths, reflecting their dominant contribution. The volume compressibility of the polyhedron follows from the behaviour of r^3, as shown in Fig. 2b. The bulk modulus of the K1 polyhedron, calculated using r^3

https://doi.org/10.1180/mgm.2025.10184 Published online by Cambridge University Press

(~6.6 GPa), agrees with the octahedral approximation value reported above (~6.5 GPa). It is worth noting that in the case of regular polyhedra with equivalent bond lengths, such as those analysed by Hazen and Finger in their derivation of Eq. 1, the volume compressibility obtained from r^3 is algebraically equivalent to that calculated directly from the polyhedral volume.

Furthermore, the use of the weighted mean bond length concept to evaluate polyhedron compressibility allows to expand the geometrical considerations discussed above in the following way:

(1) When the central cation is less compressible than the ligand anions, upon compression, its first coordination sphere tends to 'expand', accommodating additional ligands from the outer coordination spheres. This leads to an increase in the weighted mean bond length and a negative steric contribution to the compressibility, which becomes lower than that predicted by Eq. 1 for a fixed coordination number.

(2) When the central cation is more compressible than the ligand anions, upon compression, its coordination sphere tends to split into two sub-shells. One of them 'collapses' to form a new coordination with a lower coordination number, while the ligands of the other are 'expelled' outside. This leads to a decrease in the weighted mean bond length and a positive steric contribution to the compressibility, which becomes higher than predicted by Eq. 1 for a fixed coordination.

The features of K^+ coordination observed in the kokchetavite structure are similar to those found in the crystal structures of leucite, nepheline, phlogopite and microcline (Table 1), i.e. those where K^+ cation occupies a relatively large and 'soft' structural cavity. *E.g.*, in the crystal structure of 1*M*-phlogopite, the K^+ cation is also 'sandwiched' between two six-membered rings of tetrahedra. Under pressure, the pressure-induced 'ditrigonalization' of these rings leads to a rapid compression of the six shortest K–O distances, from ~2.95 Å at 1 atm to ~2.7 at 6 GPa (Fig 3a). However, the six distances to 'outer' oxygen ligands only decrease by less than 0.1 Å, leading to a decrease in *ECoN* from ~10 to ~8 (Fig. 3b).

https://doi.org/10.1180/mgm.2025.10184 Published online by Cambridge University Press

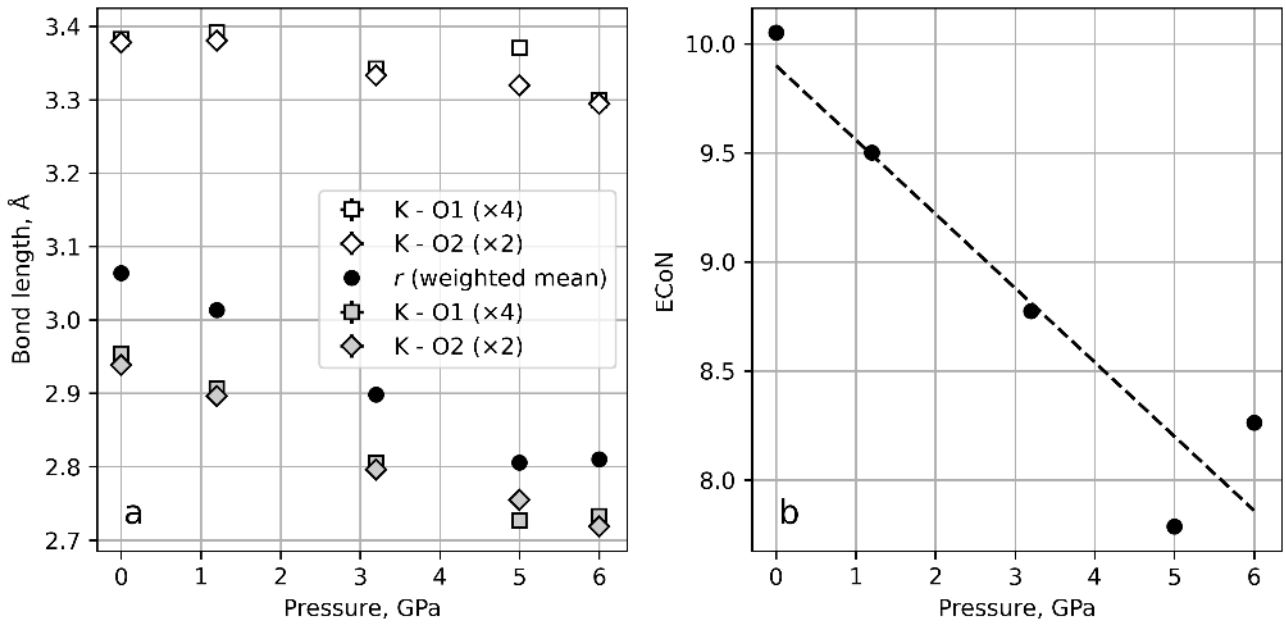

Figure 3. Parameters of K^+ site coordination in the phlogopite structure under compression. Grey and white symbols represent the six nearest ligands and the six 'outer' ligands, respectively. Black circles in (a) indicate the weighted mean distance, and dashed lines in (b) represent a least squares fit using a linear function.

Another example is the crystal structure of leucite. In this structure, the '6 + 6' coordination of the K^+ site is composed of six nearest neigbours at a distance between 2.8 and 3.2 Å, and six neighbours at a further distance of between 3.4 and 3.8 Å. These latter neighbours complement the one-sided coordination by the former, as shown in Fig. 4.

https://doi.org/10.1180/mgm.2025.10184 Published online by Cambridge University Press

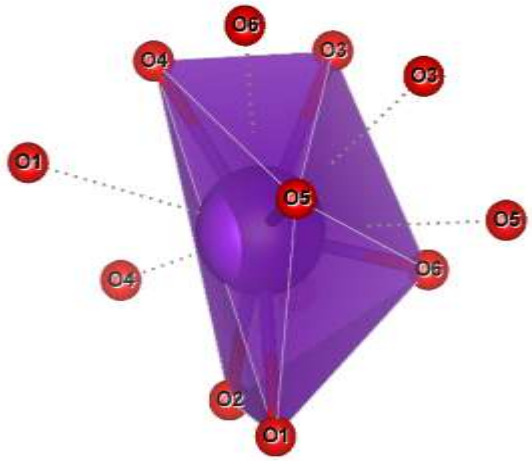

Figure 4. Coordination of the K^+ site in the crystal structure of leucite at 1 atm. The bonds to the six nearest (2.8-3.2 Å) neighbours are shown as cylinders, and the bonds to the next six neighbours (3.4-3.8 Å) are shown as dotted lines.

Upon compression up to 1.8 GPa, the six 'outer' bonds are again almost insensitive to pressure, so that their average distance decreases by only ~0.02 Å or ~0.6% (Fig. 5). The six closest bonds, however, demonstrate several times higher compression, by ~0.09 Å or ~3%. As a result, the bond weights of the 'outer' ligands decrease, as well as *ECoN* (Fig. 5b).

https://doi.org/10.1180/mgm.2025.10184 Published online by Cambridge University Press

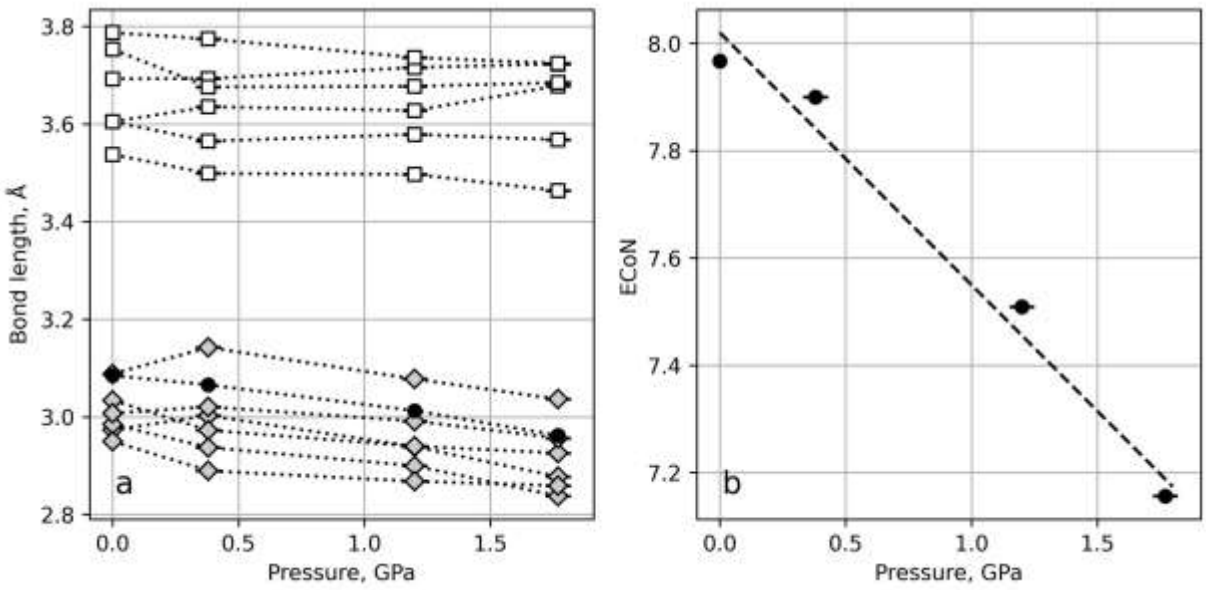

Figure 5. Parameters of K^+ site coordination in the leucite structure under compression. Grey diamonds and white squares represent to the six nearest and six 'outer' ligands, respectively. Black circles in (a) indicate the weighted mean distance. The dashed line in (b) represent a least squares fit using a linear function.

Steric contribution into compressibility of K^+ polyhedra

A systematic analysis of available data on the compressibility of K–O polyhedra (Table 1) confirms the above conclusions. Specifically, K^+ polyhedra with nearly fixed coordination (i.e., $d(ECoN) / dP \approx 0$) exhibit compressibility close to that predicted by Eq. 1 (Fig. 6a). In contrast, polyhedra with significant pressure-induced changes in coordination (i.e., $d(ECoN) / dP < 0$) show higher compressibility than predicted by Eq. 1 due to the additional steric contribution discussed above (Fig. 6a). It is not surprising that the deviation from Eq. 1 is proportional to $d(ECoN) / dP$ (Fig. 6a), which quantifies how readily the inner coordination shell collapses upon compression. The $d(ECoN) / dP$ value itself appears to be a function of the weighted mean bond length (Fig. 6b), such that K^+ polyhedra with r_0 below ~3.0 Å tend to maintain their initial coordination, while those with larger r_0 tend to collapse upon compression.

https://doi.org/10.1180/mgm.2025.10184 Published online by Cambridge University Press

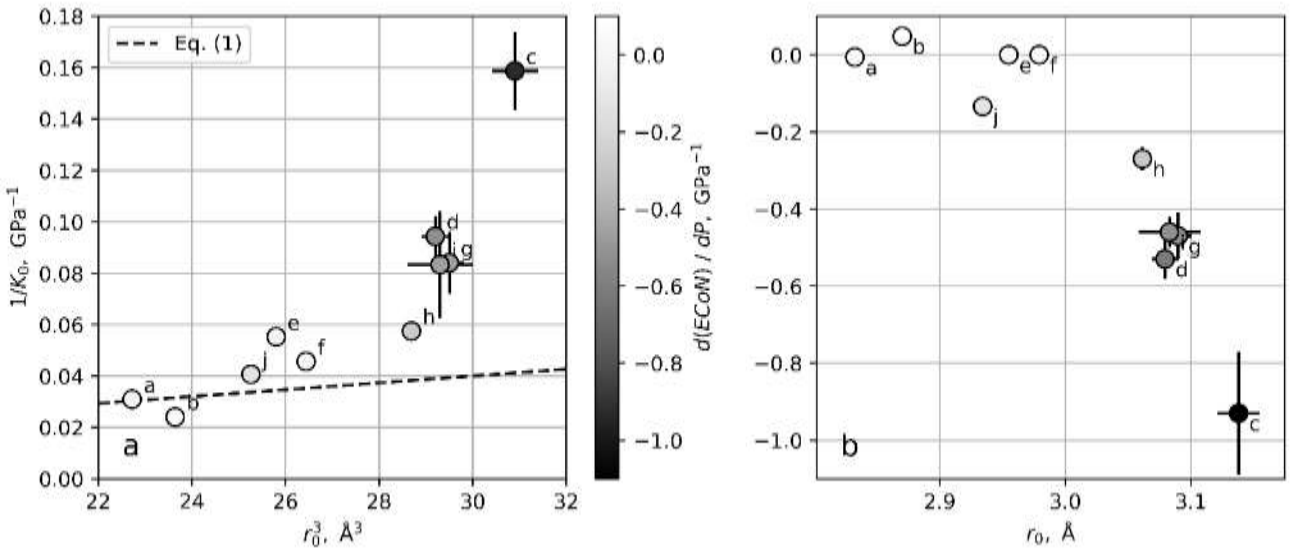

Figure 6. (a) Plot of compressibility vs. volume for K^+ polyhedra, obtained using r^3. The dashed line represents Eq. 1. (b) Dependence of the d(*ECoN*) / d*P* derivative on r_0. The colour in (a) and (b) indicates the value of d(*ECoN*) / d*P*. The small letters correspond to the 'key' column in Table 1.

Although the above considerations provide a qualitative explanation for the experimental data, it may also be interesting to quantify the steric contribution to the compressibility of polyhedra. In terms of the relative change in r^3, let us consider the 'pure' pressure contribution, which corresponds to the bond compression at a fixed coordination, following Eq. 1. We can also consider the steric contribution, which corresponds to an 'expansion' or 'collapse' of r^3 due to a gradual change in the effective coordination number:

$$dr^3/r^3 = \left(\frac{\partial r^3/r^3}{\partial P}\right)_{ECoN} \cdot dP + \left(\frac{\partial r^3/r^3}{\partial ECoN}\right)_P \cdot d(ECoN). \quad (2)$$

When the effective coordination number itself depends on pressure, it follows

$$dr^3/r^3 = \left(\frac{\partial r^3/r^3}{\partial P}\right)_{ECoN} \cdot dP + \left(\frac{\partial r^3/r^3}{\partial ECoN}\right)_P \cdot \frac{d(ECoN)}{dP} \cdot dP \quad (3)$$

$$\frac{dr^3/r^3}{dP} = \left(\frac{\partial r^3/r^3}{\partial P}\right)_{ECoN} + \left(\frac{\partial r^3/r^3}{\partial ECoN}\right)_P \cdot \frac{d(ECoN)}{dP}, \quad (4)$$

or

$$\beta = \beta_P + \beta_{ECoN}, \quad (5)$$

where

$$\beta = -\frac{dr^3/r^3}{dP} = \frac{1}{K}, \quad (6)$$

https://doi.org/10.1180/mgm.2025.10184 Published online by Cambridge University Press

$$\beta_P = -(\frac{\partial r^3/r^3}{\partial P})_{ECoN}, (7)$$

and

$$\beta_{ECoN} = -(\frac{\partial r^3/r^3}{\partial ECoN})_P \cdot \frac{d(ECoN)}{dP} \qquad (8)$$

are overall compressibility (β) and its pressure (β_P) and steric (β_{ECoN}) parts.

Since the first derivative in Eq. 8 is positive, the sign of the steric contribution β_{ECoN} will depend on the slope of d(*ECoN*) / d*P*. When the effective coordination number decreases with pressure, i.e. when the cation exhibits higher compressibility than the ligands, the overall compressibility will be higher than predicted by the Eq. 1, and vice versa.

Although the steric contribution to polyhedron compressibility can be estimated simply as the difference between the measured 1 / *K* value for r^3 and the value predicted by Eq. 1, it is also interesting to evaluate in independently from the observed d(*ECoN*) / d*P* value. For this evaluation, a value of the first derivative in Eq. 8 is needed, which corresponds to the relative change in polyhedron volume caused by a change in the number of ligands. Although this value is geometry-specific, reasonable approximations can be made. E.g., for coordination numbers between eight and 12, linear interpolation between r^3 values for a regular cube (*ECoN* = 8) and a cuboctahedron (*ECoN* = 12), assuming a fixed distance between neighbouring ligands, gives

$$\frac{\partial r^3/r^3}{\partial ECoN} \approx \frac{1}{ECoN-0.59}, (9)$$

which corresponds to a value of ~0.11 at *ECoN* = 10. The empirical data yield a similar average value of 0.09(3) within the analysed *ECoN* range (Fig. 7a), although the data scatter makes it difficult to discuss the exact dependence on effective the coordination number.

https://doi.org/10.1180/mgm.2025.10184 Published online by Cambridge University Press

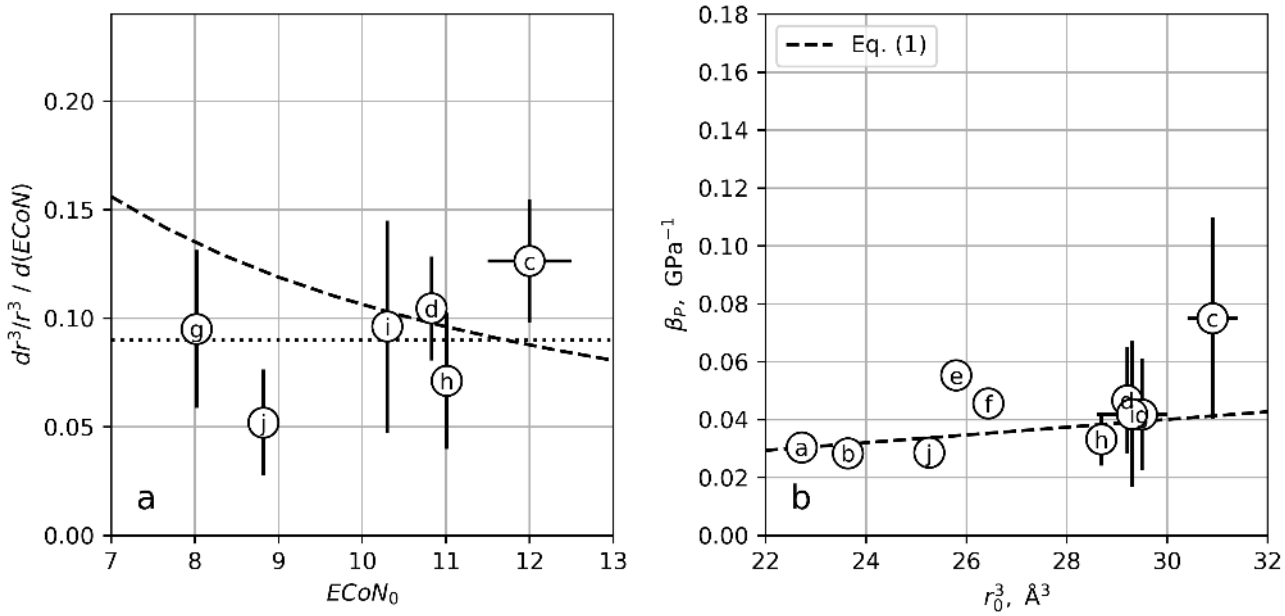

Figure 7. (a) The derivative dr^3/r^3 / d(*ECoN*) vs. $ECoN_0$ calculated using Eq. 8. The data with |d(*ECoN*) / d*P*| < 0.1 was omitted to avoid propagating large uncertainties. The dotted line represents an average value of 0.09(3) and the dashed line is the linear interpolation between the regular cube and the cuboctahedron, as described in the text. (b) The pressure contribution β_P to the overall compressibility of K^+ polyhedra. The dashed line represents Eq. 1. The small letters correspond to the 'key' column in Table 1.

The obtained dr^3/r^3 / d(*ECoN*) value of 0.09(3) allows to independently evaluate the steric contribution β_{ECoN} to the overall compressibility using Eq. 8, and then subtract this value to obtain the 'pure' pressure contribution β_P. The resulting values (Fig. 7b) are in reasonable agreement with Eq. 1 indicating a general suitability of the proposed approach.

Conclusions

A difference in the compressibility of a central ion and its ligands can lead to a continuous pressure-induced change in coordination. This should be examined by the plotting effective coordination number vs. pressure curves. A decrease in the effective coordination number (*ECoN*) with pressure can lead to the splitting and 'collapse' of the coordination sphere, creating an additional (steric) contribution to the overall volume compressibility of the coordination polyhedron. When the *ECoN* changes with pressure, the traditional methods of analysing polyhedron compressibility based on its geometric volume can be misleading. Instead, it is

https://doi.org/10.1180/mgm.2025.10184 Published online by Cambridge University Press

recommended to use weighted mean bond lengths and their cubes as measures of the linear and volume compressibilities of polyhedra for unbiased analysis.

The proposed formalism, which separates 'pure' pressure and steric contributions to polyhedral compressibility, is, on the one hand, fully consistent with traditional treatments of polyhedral compressibility at fixed coordination, and on the other hand, provides a new versatile tool for high-pressure crystal chemistry. Some promising applications of this formalism include:

(1) The high-pressure behaviour of small cations, such as Si^{4+}, Al^{3+}, B^{3+} and C^{4+}, which may exhibit continuous transitions between four-, five- and six-fold coordination, or three- and four-fold coordination.

(2) High-pressure structural chemistry of glasses and melts, especially those containing small cations listed in the previous point. While the traditional concept uses geometric volumes of polyhedra that are barely accessible for experimental studies of disordered systems, averaged parameters such as *ECoN* and the weighted mean bond length can, in principle, be directly extracted from pair distribution functions obtained either experimentally or using molecular dynamics simulations.

Acknowledgements

The work was supported by the Russian Science Foundation (grant No. 23-77-10047).

Competing interests

The author declares none.

References

Allan D.R. and Angel R.J. (1997) A high-pressure structural study of microcline ($KAlSi_3O_8$) to 7 GPa. European Journal of Mineralogy, **9**, 263–276.

Comodi P., Fumagalli P., Montagnoli M. and Zanazzi P.F. (2004) A single-crystal study on the pressure behavior of phlogopite and petrological implications. American Mineralogist, **89**, 647–653.

Downs R.T. and Hall-Wallace M. (2003) The American Mineralogist crystal structure database. American Mineralogist, **88**, 247–250.

Gatta G.D. and Angel R.J. (2007) Elastic behavior and pressure-induced structural evolution of nepheline: Implications for the nature of the modulated superstructure. American Mineralogist, **92**, 1446–1455.

https://doi.org/10.1180/mgm.2025.10184 Published online by Cambridge University Press

Gatta G.D., Rotiroti N., Ballaran T.B. and Pavese A. (2008) Leucite at high pressure: Elastic behavior, phase stability, and petrological implications. American Mineralogist, **93**, 1588–1596.

Hazen R.M. and Finger L.W. (1979) Bulk modulus—volume relationship for cation-anion polyhedra. Journal of Geophysical Research: Solid Earth, **84**, 6723–6728.

Hazen R.M. and Prewitt C.T. (1977) Effects of temperature and pressure on interatomic distances in oxygen-based minerals. American Mineralogist, **62**, 309–315.

Hoppe R. (1979) Effective coordination numbers (*ECoN*) and mean fictive ionic radii (MEFIR). Zeitschrift für Kristallographie – Crystalline Materials, **150**, 23–52.

Ignatov M.A., Rashchenko S.V., Likhacheva A.Y., Romanenko A.V., Shatskiy A.F., Arefiev A.V. and Litasov K.D. (2024) High-pressure structural behavior of α-$K_2Ca_3(CO_3)_4$ up to 20 GPa. Physics and Chemistry of Minerals, **51**, 30.

Nespolo M., Ferraris G. and Ohashi H. (1999) Charge distribution as a tool to investigate structural details: meaning and application to pyroxenes. Acta Crystallographica Section B: Structural Science, **55**, 902–916.

Rashchenko S.V. (2025) *crystchemlib* : a Python library and GUI for analysis of crystal structure datasets. Journal of Applied Crystallography, **58**, 290–295.

Romanenko A.V., Rashchenko S.V., Korsakov A.V., Sokol A.G. and Kokh K.A. (2024) Compressibility and pressure-induced structural evolution of kokchetavite, hexagonal polymorph of $KAlSi_3O_8$, by single-crystal X-ray diffraction. American Mineralogist, **109**, 1284–1291.

Seryotkin Y.V. (2024) Structure evolution of hydroxyapophyllite-(K) under high pressure. Physics and Chemistry of Minerals, **51**, 3.

Seryotkin Y.V. and Ignatov M.A. (2023) Structure evolution of fluorapophyllite-(K) under high pressure. High Pressure Research, **43**, 279–292.

https://doi.org/10.1180/mgm.2025.10184 Published online by Cambridge University Press